

Transcriptome and epigenome analyses of vernalization in *Arabidopsis thaliana*

Yanpeng Xi, Sung-Rye Park¹, Dong-Hwan Kim² , Eun-Deok Kim and Sibum Sung* 

Department of Molecular Biosciences and The Institute for Cellular and Molecular Biology, The University of Texas at Austin, Austin, TX, 78712, USA

Received 25 February 2020; revised 24 April 2020; accepted 5 May 2020; published online 15 May 2020.

*For correspondence (e-mail sbsung@austin.utexas.edu).

¹Present address: Department of Molecular and Integrative Physiology, University of Michigan, Ann Arbor, MI, USA

²Present address: Department of Plant Science and Technology, Chung-Ang University, Anseong, Korea

SUMMARY

Vernalization accelerates flowering after prolonged winter cold. Transcriptional and epigenetic changes are known to be involved in the regulation of the vernalization response. Despite intensive applications of next-generation sequencing in diverse aspects of plant research, genome-wide transcriptome and epigenome profiling during the vernalization response has not been conducted. In this work, to our knowledge, we present the first comprehensive analyses of transcriptomic and epigenomic dynamics during the vernalization process in *Arabidopsis thaliana*. Six major clusters of genes exhibiting distinctive features were identified. Temporary changes in histone H3K4me3 levels were observed that likely coordinate photosynthesis and prevent oxidative damage during cold exposure. In addition, vernalization induced a stable accumulation of H3K27me3 over genes encoding many development-related transcription factors, which resulted in either inhibition of transcription or a bivalent status of the genes. Lastly, *FLC*-like and *VIN3*-like genes were identified that appear to be novel components of the vernalization pathway.

Keywords: vernalization, transcriptome, histone modification, RNA-seq, ChIP-seq, *Arabidopsis*.

INTRODUCTION

Temperature is an important environmental cue that, coupled with day length, cues plants to initiate flowering. For most winter annual and biennial plants, the prevention of flowering before winter and induction of flowering after winter is required for successful reproduction. Cold itself is not sufficient, as temperature fluctuations in the fall might be falsely taken as the passing of winter. A timing mechanism is needed to distinguish long-term winter cold exposure from short-term chilling stress. Therefore, the vernalization process evolved, which accelerates flowering only after prolonged cold exposure. In winter-annual *Arabidopsis thaliana*, vernalization is regulated by two major loci: *FLOWERING LOCUS C (FLC)* and *FRIGIDA (FRI)* (Shindo *et al.*, 2005; Werner *et al.*, 2005; Coustham *et al.*, 2012). *FLC* encodes a MADS-box transcription factor that represses the expression of downstream targets (Michaels and Amasino, 1999; Hepworth *et al.*, 2002; Lee and Lee, 2010). *FRI* acts with other proteins in a complex to upregulate *FLC* expression (Johanson *et al.*, 2000; Choi *et al.*, 2005; Schmitz *et al.*, 2005; Kim *et al.*, 2006; Geraldo *et al.*, 2009; Jiang *et al.*, 2009;

Hu *et al.*, 2014; Li *et al.*, 2018). A high level of *FLC* and its clade members prevent flowering by repressing floral integrator genes such as *FLOWERING LOCUS T (FT)* and *SUPPRESSOR OF OVEREXPRESSION OF CONSTANS 1 (SOC1)* (Sheldon *et al.*, 2000; Hepworth *et al.*, 2002; Moon *et al.*, 2003; Michaels *et al.*, 2005; Helliwell *et al.*, 2006; Searle *et al.*, 2006; Gu *et al.*, 2013) and feedback regulations operate between *FLC* and floral integrators (Chen and Penfield, 2018; Luo *et al.*, 2019), forming intricate regulatory networks that control flowering. *FLC* is stably repressed by prolonged winter cold, thereby enables rapid induction of flowering under favorable day length in spring. The vernalization-triggered *FLC* repression is mitotically stable and it is reset only during meiosis to ensure the requirement of vernalization in the next generation (Sheldon *et al.*, 2008). This “memory” of winter indicates the involvement of epigenetic regulation. Indeed, studies performed during the past decade have begun to elucidate the role of histone modification and chromatin structural dynamics in *FLC* repression (Sung and Amasino, 2004; Mylne *et al.*, 2006; Sung and Amasino, 2006; Sung *et al.*, 2006; De Lucia *et al.*, 2008; Kim

et al., 2010; Heo and Sung, 2011; Crevillen *et al.*, 2013; Rosa *et al.*, 2013; Questa *et al.*, 2016; Kim and Sung, 2017).

Before vernalization, *FLC* chromatin is enriched with active histone marks, including histone acetylation, H3K4me3 and H3K36me3, which are likely deposited by FRI complexes (Kim *et al.*, 2005; Schmitz *et al.*, 2005; Jiang *et al.*, 2009; Tamada *et al.*, 2009; Whittaker and Dean, 2017). Early in vernalization, the expression of antisense non-coding RNAs are induced at the *FLC* locus. Expression of these RNAs, termed *cold-induced long antisense intragenic RNA (COOLAIR)* correlates with the reduction in expression of the *FLC* sense transcript, and *COOLAIR* physically associates with *FLC* chromatin resulting in depletion of H3K36me3 (Swiezewski *et al.*, 2009; Csorba *et al.*, 2014). Recently, expression of *VP1/ABI3-LIKE1 (VAL1)* was shown to be necessary for vernalization-mediated reduction of histone acetylation at *FLC*. *VAL1* is a B3 domain protein recruited to *FLC* through its direct binding to RY motifs within the nucleation region. *VAL1* recruits histone deacetylase HDA19 to *FLC* chromatin (Questa *et al.*, 2016; Yuan *et al.*, 2016).

In the late stage of vernalization, prolonged cold induces a sufficient amount of VERNALIZATION INSENSITIVE 3 (*VIN3*), a PHD-finger domain protein, which forms a heterodimer with *VIN3-LIKE 1 (VIL1)* and together recruit POLYCOMB REPRESSIVE COMPLEX 2 (*PRC2*) to the nucleation region in the first intron of *FLC*. This PHD-*PRC2* complex catalyzes the tri-methylation of histone H3K27, a well-characterized repressive mark (De Lucia *et al.*, 2008). At this stage, H3K27me3 modifications are confined within the nucleation region. Meanwhile, expression of another non-coding RNA, termed *cold-assisted intronic non-coding RNA (COLDAIR)* is induced from the sense direction of the first intron of *FLC*. Loss of *COLDAIR* results in a vernalization-insensitive phenotype (Heo and Sung, 2011). *COLDAIR* interacts with CURLY LEAF (*CLF*), the enzymatic core of *PRC2*, to facilitate its sequence-specific binding at the *FLC* locus (Heo and Sung, 2011; Kim and Sung, 2017). When temperatures warm, *VIN3* levels decline rapidly, but *VIL1-PRC2* remains bound to the *FLC* locus. H3K27me3 spreads until it covers the entire genomic region of *FLC*. It is not clear how or why the spreading of repressive marks occurs only when the temperature warms. The accelerated enzymatic activity of histone-modifying complexes at higher temperatures might explain this phenomenon. LIKE HETEROCHROMATIN PROTEIN 1 (*LHP1*) proteins are enriched at *FLC* following *PRC2* action, and these proteins are necessary for stable maintenance of the epigenetically repressed state of *FLC* in warm conditions. *VAL1* recruits *LHP1* to *FLC* through direct protein-protein interactions (Yuan *et al.*, 2016). The repressive state of *FLC* is stably inherited through many cycles of cell division during subsequent growth and development.

In addition to changes in histone modifications, chromatin structural changes also occur at the *FLC* locus during vernalization. Vernalization induces physical clustering of *FLC* alleles in the nucleus, which requires Polycomb complex components VERNALIZATION INSENSITIVE 2 (*VRN2*) and *VIL1*, but not *LHP1* (Rosa *et al.*, 2013). An interaction between the 5' and 3' regions of the *FLC* chromatin is formed before cold exposure and is disrupted during the early stage of vernalization. The mechanism of formation of this loop is not clear. It is known that the transcriptional status of *FLC* is not relevant to this process and that the components of *PRC2* complex are not necessary (Crevillen *et al.*, 2013). An intragenic chromatin loop is also induced by vernalization, which could be responsible for the vernalization-induced spreading of H3K27me3 marks along the *FLC* chromatin (Kim and Sung, 2017). A non-coding RNA derived from the *FLC* promoter called *COLDWRAP* (also known as *cold of winter-induced noncoding RNA from the promoter*) is involved in the formation of the intragenic chromatin loop.

Given the quantitative nature of the vernalization response, it would be helpful to have a comprehensive picture of the transcriptome and epigenome changes that occur during the vernalization process. To date, few vernalization-related next-generation sequencing datasets have been generated, and most come from food crops such as pak choi (*Brassica rapa* subsp. *chinensis*) and radish (*Raphanus sativus* L.) (Sun *et al.*, 2015; Liu *et al.*, 2016). The RNA-seq and ChIP-seq analyses collected at multiple time points during vernalization described in this work represent the first comprehensive profiling of the transcriptome and epigenome dynamics of vernalization in *A. thaliana*.

RESULTS

Transcriptional dynamics of vernalization in *Arabidopsis thaliana*

To capture genome-wide transcriptional dynamics during the vernalization process, seven samples were collected, termed NV (without cold exposure), V1h (1-h cold), V1d (1-day cold), V10d (10-day cold), V20d (20-day cold), V40d (40-day cold) and T10 (40-day cold followed by 10-day normal growth temperature). The well-known patterns of *FLC* repression and *VIN3* induction were successfully captured by the RNA-seq (Figure 1a,b and Table S1). *FLC* belongs to a small gene family, including *FLC* and the *MADS AFFECTING FLOWERING* genes *MAF1* (also known as *FLOWERING LOCUS M*), *MAF2*, *MAF3*, *MAF4* and *MAF5*. The RNA-seq data showed relatively similar dynamics of *MAF1* and *FLC* that differed from the patterns of expression of *MAF2* and *MAF3* (Figure 1a). *MAF4* and *MAF5* were of too low abundance for a pattern of expression to be confidently differentiated by RNA-seq. Of the *VIN* family members, *VIL2*

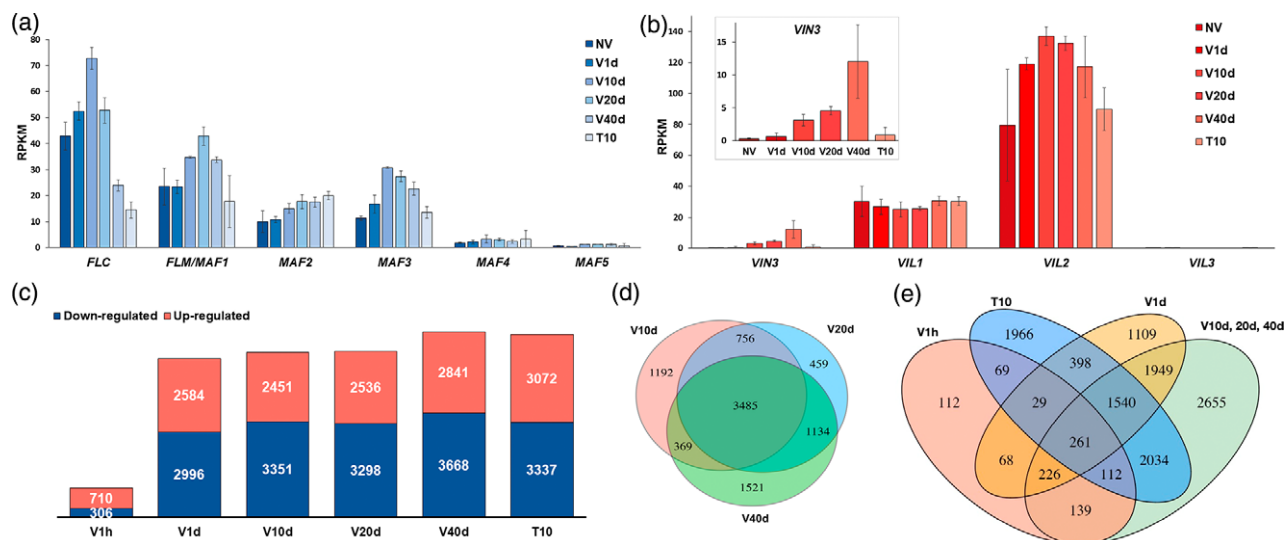


Figure 1. Changes in the *Arabidopsis* transcriptome during the course of vernalization.

(a) Quantitative measurement of expression levels of *FLC* family genes over a time course during vernalization as in reads per kilobase of transcript, per million mapped reads (RPKM). Error bars were generated based on normalized read counts within each locus from two biological replicates. (b) Quantitative measurement of expression levels of *VIN3* family genes over a time course during vernalization as in RPKM. Error bars were generated based on normalized read counts within each locus from two biological replicates. NV, without cold exposure; V1h, 1-h cold; V1d, 1-day cold; V10d, 10-day cold; V20d, 20-day cold; V40d, 40-day cold; T10, 40-day cold followed by 10-day normal growth temperature. (c) Bar graph showing total numbers of differentially upregulated (red) and downregulated (blue) genes at each time point relative to NV. (d) Venn diagram showing the overlapping and uniquely differentially regulated genes at V10d, V20d and V40d. (e) Venn diagram showing the overlapping and uniquely differentially regulated genes at V1h, V1d, V10d/20d/40d and T10.

showed the highest expression, whereas *VIL3* was barely detected. Levels of *VIL1* and *VIL2* were largely stable across vernalization (Figure 1b).

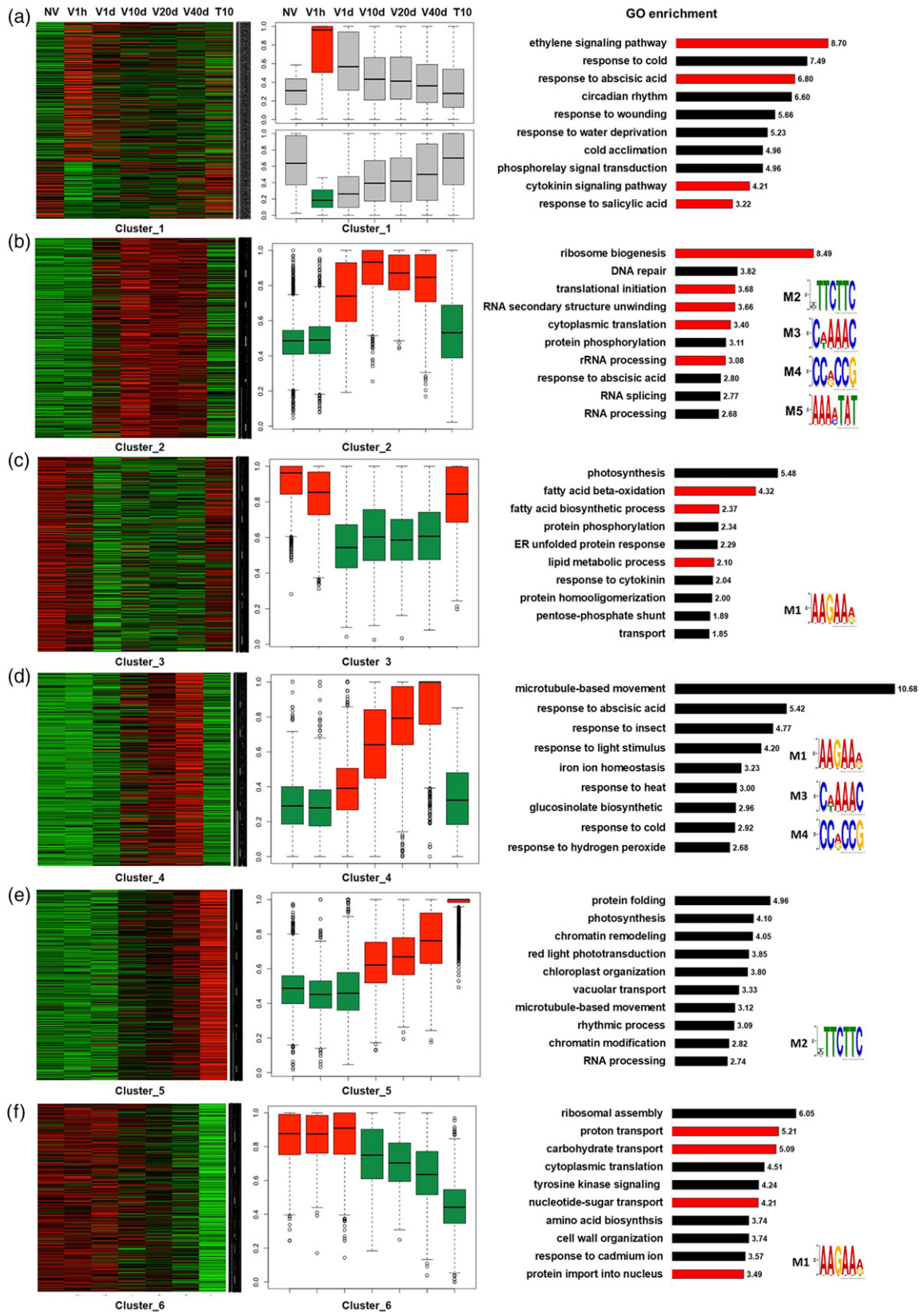
Differentially expressed genes were by comparison of vernalized samples to NV samples. All the time points, except V1h, showed similar numbers of up- and down-regulated genes (Figure 1c). Only 710 upregulated and 306 downregulated genes were identified in V1h samples, indicating that the downstream cascades of cold-regulated genes were initiated by a limited number of early responsive genes. V10d, V20d and V40d shared 3485 differentially regulated genes in common (Figure 1d), suggesting that expression of many cold-regulated genes was stably maintained regardless of the duration of cold. That 3976 of the 5580 genes expressed during V1d were also expressed at one or more of the V10d, V20d and V40d time points indicate that long-term responses built up within just 1 day of cold exposure are maintained (Figure 1e).

To explore the time-course dynamics fully, differentially expressed genes from all time points were clustered based

on expression patterns. Six major clusters with distinct transcriptional dynamics were identified (Figure 2). Cluster 1 consisted of a small number of early responsive genes (545) that were up- or downregulated within just 1 h of cold treatment (Figure 2a). Gene ontology (GO) analysis revealed that this cluster was enriched in hormone-related genes, including ethylene, abscisic acid, cytokinin and salicylic acid (Figure 2a), which is consistent with the fact that plant hormones are usually among the “first responders” upon environmental changes and stresses. Members of cluster 2 (2272 genes) and cluster 3 (1744 genes) exhibited relatively constant up- and downregulation, respectively, at time points V1d–V40d (Figure 2b,c), indicating that these genes are regulated during cold. GO analysis showed that upregulated genes in cluster 2 were enriched in translation-related terms (Figure 2b), such as ribosome biogenesis, translation initiation, RNA secondary structure unwinding and rRNA processing, suggesting that protein synthesis is boosted during prolonged cold, probably to make up for the reduced enzymatic activity at low temperature.

Figure 2. Clustering analysis of transcriptome data collected during vernalization.

(a–f) Clusters 1–6, respectively, were generated from *k*-means clustering of transcription profiles obtained over the time course of vernalization. Shown from left to right for genes in the indicated cluster are heatmaps of gene expression at each time point, normalized box plots of genes expression at each time point, enriched gene ontology (GO) terms, and motifs enriched within clustered genes if detected. In normalized box plots of gene expression: gray boxes, no significant difference; red boxes, significant upregulation; green boxes, significant downregulation. NV, without cold exposure; V1h, 1-h cold; V1d, 1-day cold; V10d, 10-day cold; V20d, 20-day cold; V40d, 40-day cold; T10, 40-day cold followed by 10-day normal growth temperature.



Photosynthesis and lipid processing genes were enriched in cluster 3 (Figure 2c), indicating that in *Arabidopsis* the photosynthesis is repressed during cold exposure. In evergreen plants, winter cold inhibits the efficiency of photosynthetic CO₂ assimilation, which could lead to overexcitation and increased photo-oxidative damage if plants continue to absorb light energy. Therefore, down-regulation of light absorption balances the supply and utilization of energy during cold exposure and protects plants from photo-oxidative damage (Oquist and Huner, 2003). Indeed, the photosynthesis-related genes in cluster 3 mostly encode components of light harvesting complexes, suggesting that *Arabidopsis* utilizes a similar strategy as evergreens during the winter cold.

Genes in cluster 4 (911 genes) had expression that was gradually induced during cold exposure instead as opposed to the constant high levels observed for genes in cluster 2 (Figure 2d). This pattern resembles that of *VIN3* during vernalization. Genes related to microtubule movement were present in this cluster. Genes in cluster 5 (1828 genes) and cluster 6 (1650 genes) had gradually increased or decreased expression during cold exposure, respectively, and levels of these genes were maintained after the return to warm temperature (Figure 2e,f). The pattern of expression of genes in cluster 6 resembled that of *FLC* during vernalization. No functional terms showed enrichment in these two clusters.

To identify potential protein-binding motifs enriched in the six major clusters, 3 kb of promoter sequences for each gene were extracted and analyzed using the MEME program for motif discovery and analysis. Five major motifs were discovered with distinct and overlapping enrichment among the clusters (Figure 2, far right; Table 1). Motif 1 (M1) was enriched in clusters 3, 4 and 6 and motif 2 (M2) in clusters 2 and 5. Motif 3 (M3) and motif 4 (M4) were

both enriched in clusters 2 and 4, and motif 5 (M5) was only enriched in cluster 2. Overall, gene clusters upregulated during vernalization showed higher motif enrichment, suggesting that the induction of genes was regulated by the combination of transcription factors, whereas repression might require distinct mechanisms. The transcription factors with binding motifs that match those enriched in genes differentially expressed during vernalization are listed in Table 2. Many of these transcription factors are involved in salt stress, hormone signaling and flowering regulation. Motif 4 was of great interest, as it is the binding motif for the ERF/AP2 transcription factors involved in hypoxia signaling (Yang *et al.*, 2011; Gasch *et al.*, 2016), and *VIN3* was reported to be induced by hypoxia (Bond *et al.*, 2009). It is also noteworthy that a recent finding showed that hypoxia also stabilizes the VRN2-containing PRC2 complex to mediate the repression of *FLC* during vernalization (Gibbs *et al.*, 2018), implicating biological relevance between hypoxia and vernalization.

Histone modification changes during vernalization

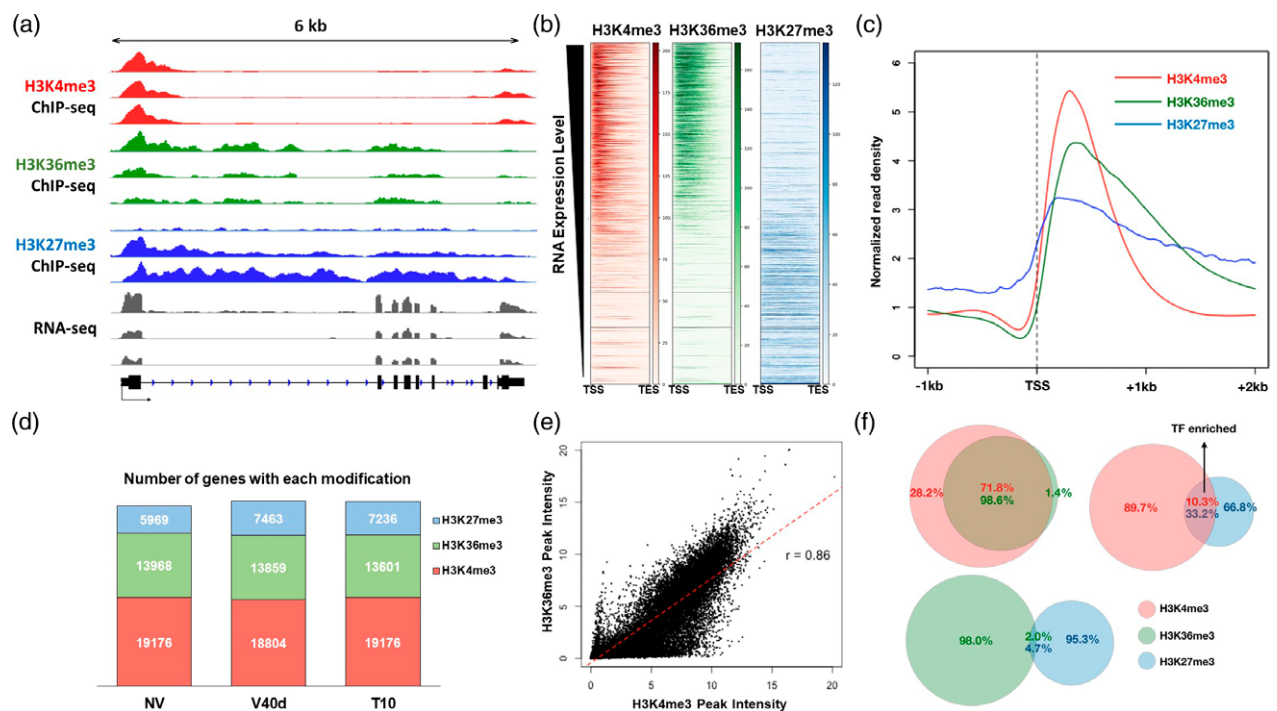
Three well-studied histone modifications, H3K27me3, H3K4me3 and H3K36me3, were analyzed by ChIP-seq at NV, V40d and T10 (Figure 3 and Table S2). We first analyzed the distribution of histone marks on *FLC* chromatin at these time points (Figure 3a). An enrichment of H3K27me3 was observed around the *FLC* transcription start site at V40d compared with NV. The gene body of *FLC* exhibited a minor increase of H3K27me3 during cold exposure, whereas the major spreading and coverage of repressive marks occurred only after plants were moved back to a warm temperature at T10 (Figure 3a). Consistent with the increase of H3K27me3, a decrease of H3K36me3 along the gene body of *FLC* was observed as a function of time, although the overall enrichment of H3K36me3 was much lower than that

	Motif 1	Motif 2	Motif 3	Motif 4	Motif 5
Cluster_2					
Cluster_3					
Cluster_4					
Cluster_5					
Cluster_6					

Table 1 Motifs enriched in each cluster of genes differentially regulated during vernalization

Table 2 Transcription factors (TFs) with binding motifs similar to those identified in genes differentially regulated during vernalization

	Motif 1 (M1)	Motif 2 (M2)	Motif 3 (M3)	Motif 4 (M4)	Motif 5 (M5)
Matched TFs	NTL4, NAC2	NTL8	CRC	ERF17, ERF38, ERF74, WIND3, WIND4	RVE1, RVE4, RVE5, RVE8, LHY, EPR1
Family	NAC domain family	NAC domain family	Plant-specific YABBY family	DREB subfamily of ERF/AP2 family	Homeodomain-like family
Reported functions		Drought response, JA biosynthesis, salt stress, embryogenesis, stamen development	Salt stress, flowering, trichome formation	Fatty acid biosynthesis, carpel development	Hypoxia response, osmotic stress, ethylene signaling, redox sensing
Circadian clock,	photoperiodic flowering, auxin signaling, chlorophyll synthesis				

**Figure 3.** Genome-wide analysis of histone modifications during the course of vernalization.

- (a) Genomic browser illustration of normalized ChIP-seq and RNA-seq results at *FLC* locus. H3K4me3 tracks are shown in red, H3K36me3 in green, and H3K27me3 in blue. RNA-seq results are shown in gray colors.
- (b) Heatmaps of H3K4me3 (red), H3K36me3 (green), and H3K27me3 (blue) over all coding genes in *Arabidopsis* genome. Each row represents the normalized read density from transcription start site to transcription end site of each gene, ranked by transcription level from the highest (top) to the lowest (bottom).
- (c) Averaged profiles of H3K4me3 (red), H3K36me3 (green), and H3K27me3 (blue) distributions around transcription start site regions over all coding genes in *Arabidopsis* genome.
- (d) Bar graph showing total number of peaks called by MACS2 within each sample. NV, without cold exposure; V40d, 40-day cold; T10, 40-day cold followed by 10-day normal growth temperature.
- (e) Correlation plot of genome-wide H3K4me3 and H3K36me3 densities.
- (f) Venn diagrams showing overlapped among different histone marks from all three time points.

of H3K27me3 at all stages. The H3K4me3 marks showed little change during and after vernalization (Figure 3a). Besides the transcription start site, a minor H3K4me3 peak was observed around the 3'-end of *FLC*. This may be involved in the formation of a chromatin loop or the expression of antisense transcripts (Swiezewski *et al.*, 2009; Csorba *et al.*, 2014). Indeed, a minor peak of H3K4me3 in 3'

FLC, as well as the localization of the H3K4 methyltransferase COMPASS (Complex Proteins Associated with Set1)-like in this region, have been reported (Li *et al.*, 2018). In addition, the 3' localized COMPASS-like appears to be involved in 5'-3' gene looping (Li *et al.*, 2018).

At the genome-wide level, H3K4me3 and H3K36me3 were enriched on actively transcribed genes, whereas

H3K27me3 was observed over genes expressed at low levels and over silenced genes (Figure 3b). H3K4me3 peaks were confined around transcription start sites with an average span of about 2 kb, whereas H3K36me3 and H3K27me3 were diffused into gene bodies (Figure 3c). Most of the H3K4me3 peaks did not change much in terms of location or intensity during vernalization (Figure 3d). H3K36me3 largely followed the pattern of H3K4me3 distribution (Figure 3e,f) as expected, as both are active histone marks. In total, 19 176, 18 804 and 19 176 peaks were called for H3K4me3 in NV, V40d and T10 samples, respectively, and 13 968, 13 859 and 13 601 peaks were called for H3K36me3 at these time points (Figure 3d). These numbers represent two-thirds of coding genes in the Arabidopsis genome, which roughly matches the number of actively transcribed genes. Thus, nearly every actively transcribed gene has an H3K4me3 peak located at their transcription start site. The lower numbers of genes marked by

H3K36me3 compared with H3K4me3 are probably due to the overall lower enrichment levels for H3K36me3 compared with H3K4me3 detected in our ChIP-seq analysis. As expected due to the synergistic function of these modifications in transcriptional regulation, 98.6% of H3K36me3 peaks overlapped with an H3K4me3 peak (Figure 3f). The H3K36me3 mark is known to prevent cryptic transcription and facilitate RNA polymerase elongation through gene bodies (Wagner and Carpenter, 2012).

A much smaller number of peaks were called for H3K27me3 than for the active histone marks, with 5969, 7463 and 7236 peaks in NV, V40d and T10 samples, respectively (Figure 3d). Only 2.0%–4.7% of peaks, depending on the time point, overlapped between the H3K36me3 and H3K27me3 marks. Surprisingly, a large portion of H3K27me3 peaks (33.2%) overlapped with the H3K4me3 marks (Figure 3f), resulting in the so-called “bivalent” status for the underlying genes (Vastenhouw and Schier,

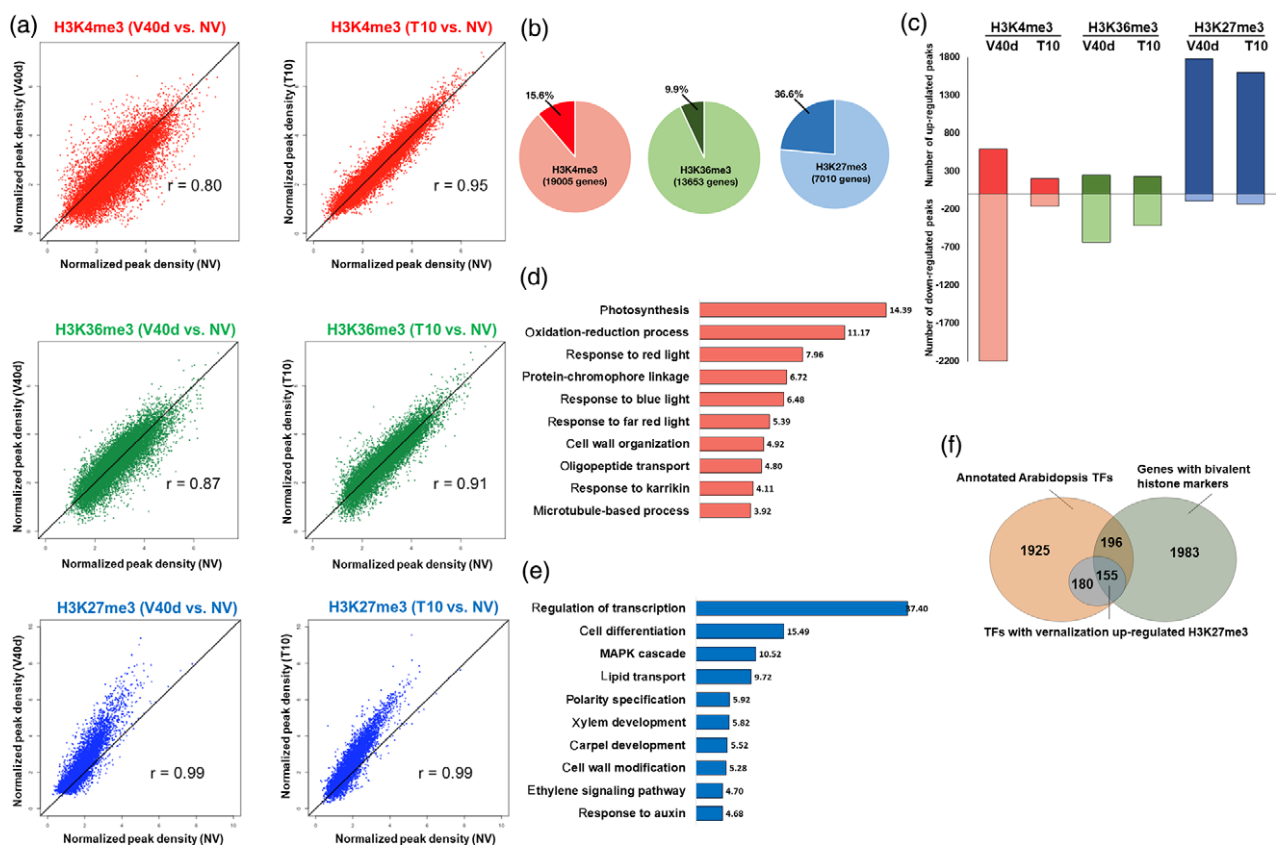


Figure 4. Characteristics of histone modification-enriched loci during the course of vernalization.

(a) Correlation plots of densities of H3K4me3 in red, H3K36me3 in green, and H3K27me3 in blue in V40d versus NV (left) and T10 versus NV (right) samples. NV, without cold exposure; V40d, 40-day cold; T10, 40-day cold followed by 10-day normal growth temperature.

(b) Pie graph showing the percentages of histone modification peaks differentially regulated during vernalization.

(c) Bar graph showing the number of vernalization upregulated (darker hues) and downregulated (lighter hues) H3K4me3 (red), H3K36me3 (green) and H3K27me3 (blue) peaks.

(d) Bar graph showing top GO terms ranked by enrichment score from H3K4me3 temporarily downregulated loci with P -value.

(e) Bar graph showing top GO terms ranked by enrichment score from H3K27me3 upregulated loci with P -value.

(f) Venn diagrams showing overlaps among all annotated transcription factors (TFs), genes with bivalent histone markers, and TFs with increased H3K27me3 by vernalization.

2012; Voigt *et al.*, 2013; Harikumar and Meshorer, 2015; Zaidi *et al.*, 2017). GO analysis indicated that transcription factors were highly enriched in the group of genes with bivalent histone marks, suggesting that the combination of H3K27me3 and H3K4me3 could be required for flexible regulation of transcription factors in *Arabidopsis*. The transcription factors with bivalent marks are listed in Table S3.

Vernalization causes an overall increase of H3K27me3 in *Arabidopsis* genome

Vernalization had minimal effect on H3K36me3 distribution, as peaks from V40d and T10 correlated well with NV samples (Figure 4a). A temporary effect of vernalization on H3K4me3 was enhanced diffusion at V40d; patterns of H3K4me3 at T10 were similar to those at NV. In contrast, vernalization-induced H3K27me3 changes observed at V40d were maintained after plants were moved back to warm temperature at T10 (Figure 4a). To quantify the differential peaks among samples, reads within each peak were extracted and converted to digital counts for statistical analysis. Consistent with the correlation analysis, only 9.9% of H3K36me3 peaks were differentially regulated; a slightly higher percentage of H3K4me3 peaks (15.6%) were differentially regulated. In contrast, over one-third of H3K27me3 peaks (36.6%) were differentially regulated by vernalization (Figure 4b). Surprisingly, the direction of change of these differentially regulated peaks was not evenly distributed: cold induced

an overall decrease of H3K4me3 and increase of H3K27me3 at V40d (Figure 4c). The absence of downregulated H3K27me3 peaks indicated a potential unidirectional action of H3K27me3 for switching off genes and suggests that, once added, the H3K27me3 mark is difficult to remove. To confirm the ChIP-seq results, several genes were randomly chosen for validation. Quantitative polymerase chain reaction (qPCR) validated the ChIP-seq analysis (Figure S1).

The group of genes with the cold-induced reduction of H3K4me3 were enriched with photosynthesis-related terms (Figure 4d), as was cluster 3 of cold downregulated genes (Figure 2c). Therefore, it is likely that in *Arabidopsis* the temporary removal of H3K4me3 marks at the transcription start site decreases the expression of photosynthesis genes to prevent photo-oxidative damage during cold exposure and quickly restores their activities in warm temperature to ensure normal growth and development. The factors involved in this temperature-induced H3K4me3 change are currently unknown.

Interestingly, transcription factors from almost all families were strongly enriched in the group of genes with H3K27me3 peaks upregulated during vernalization (Figure 4e). In addition, of the 335 transcription factor genes that had strongly upregulated H3K27me3, 155 were marked with H3K4me3 (Figure 4f). GO analysis revealed that floral regulator genes were enriched in the group of transcription factors with vernalization-induced H3K27me3 modifications (Table 3), confirming that vernalization promotes the transition from vegetative growth to reproductive growth through epigenetic switching off of regulatory hub genes in *Arabidopsis*.

Table 3 Functional annotations of transcription factors with vernalization-induced H3K27me3 upregulation

Functional annotation	Number of genes	Enrichment score	P-value
Cell differentiation	59	40.82	1.30E-13
Ethylene signaling pathway	30	17.4	1.00E-19
Flower development	25	11.12	2.20E-13
Carpel development	10	9.4	1.30E-11
Ovule development	11	6.85	5.40E-09
Regulation of secondary cell wall biogenesis	8	6.82	5.20E-09
Vegetative to reproductive phase transition of meristem	14	6.1	3.30E-08
Gibberellic acid signaling pathway	11	4.82	6.50E-07
Specification of flora organ identity	6	4.57	1.30E-06
Trichome differentiation	7	4.32	2.40E-06
Transmitting tissue development	4	3.42	2.20E-05
Auxin signaling pathway	14	3.21	3.80E-05

Identification of *FLC*-like and *VIN3*-like transcripts

We hypothesized that any gene with a repression pattern similar to that of *FLC* or an induction pattern similar to that of *VIN3* upon cold treatment could have similar functions during vernalization. Clusters 6 and 4 included genes with patterns of expression similar to those of *FLC* and *VIN3*, respectively (Figure 2d,f). A dynamic time warping (DTW) algorithm was used to identify optimal matches within each cluster. DTW was first used in speech recognition for measuring the similarity between soundtracks (Sakoe and Chiba, 1978). The advantage of DTW over simple pairwise comparison is that it allows the stretch and compression of input sequences. In this work, the time-series transcriptional dynamics of two genes were given as inputs, and a distance score was then calculated (Figure 5a,b). The lower the distance score, the higher the similarity of the two expression patterns (Figure 5b).

All genes within cluster 6 were compared with *FLC* using DTW, and the resulting distance scores were ranked from low to high (Figure 5c). Genes in cluster 4 genes were ranked for similarity to the *VIN3* expression pattern

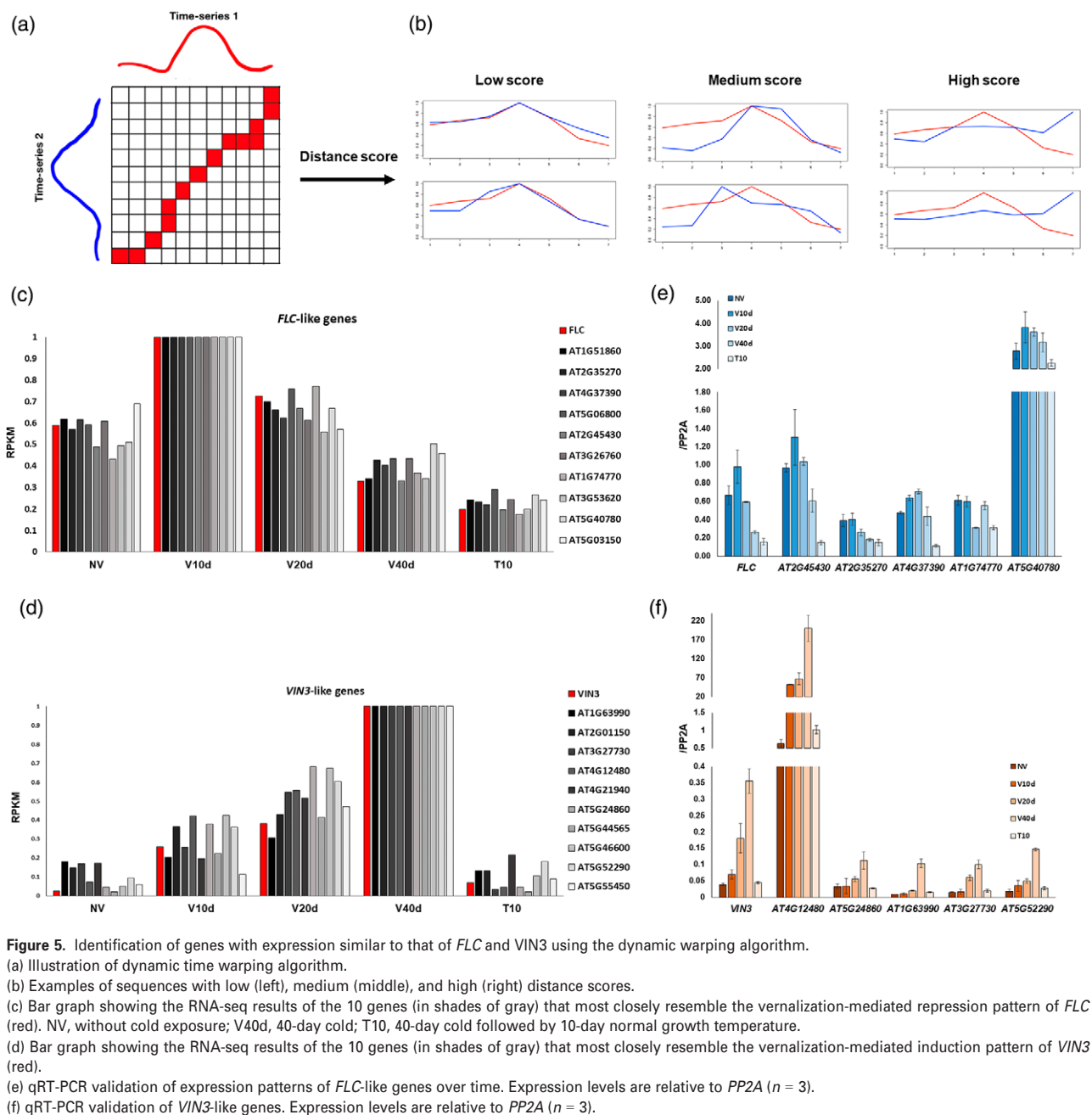


Figure 5. Identification of genes with expression similar to that of *FLC* and *VIN3* using the dynamic warping algorithm.

(a) Illustration of dynamic time warping algorithm.

(b) Examples of sequences with low (left), medium (middle), and high (right) distance scores.

(c) Bar graph showing the RNA-seq results of the 10 genes (in shades of gray) that most closely resemble the vernalization-mediated repression pattern of *FLC* (red). NV, without cold exposure; V40d, 40-day cold; T10, 40-day normal growth temperature.

(d) Bar graph showing the RNA-seq results of the 10 genes (in shades of gray) that most closely resemble the vernalization-mediated induction pattern of *VIN3* (red).

(e) qRT-PCR validation of expression patterns of *FLC*-like genes over time. Expression levels are relative to *PP2A* ($n = 3$).

(f) qRT-PCR validation of *VIN3*-like genes. Expression levels are relative to *PP2A* ($n = 3$).

(Figure 5d). To validate the transcriptional profiles of the *FLC*- and *VIN3*-like genes identified from the DTW algorithm, transcripts from five genes from each category were quantified in time-course samples. The results of qRT-PCR were consistent with the RNA-seq profiles (Figure 5e,f). Several of the *FLC*- and *VIN3*-like genes are known floral regulators and cold-related genes that could be novel components of the vernalization pathway (Tables 4 and 5). Interestingly, of the top 10 *VIN3*-like genes, three encode factors involved in meiotic recombination (Table 5), suggesting that *VIN3* may have a role in meiotic recombination or may regulate chromatin contact.

AHL family genes act as floral repressors in vernalization pathway

In the set of 10 most *FLC*-like genes were two AT-hook family genes, *AT-HOOK MOTIF NUCLEAR LOCALIZE PROTEIN 21 (AHL21)* and *AT-HOOK MOTIF NUCLEAR LOCALIZE PROTEIN 22 (AHL22)*. qRT-PCR confirmed their expression patterns (Figure 6b). As found in our analysis of *FLC*, stable increases of H3K27me3 were observed on both loci during and after vernalization (Figure 6a). Previous studies have shown that *AHL* family genes are involved in the control of flowering (Ng *et al.*, 2009; Xiao

Table 4 Genes with expression patterns similar to *FLC* during the course of vernalization

Locus	Name	Protein domain	Reported function
AT1G51860	–	LRR, protein kinase	–
AT2G45430	AHL22	AT-hook DNA-binding	Regulation of flowering
AT2G35270	AHL21	AT-hook DNA-binding	Patterning and differentiation of reproductive organs
AT4G37390	AUR3	GH3 auxin-responsive	Negative component in auxin signaling
AT5G06800	–	Myb-like DNA-binding	–
AT3G26760	–	Glucose dehydrogenase	–
AT1G74770	BTSL1	Zinc finger	Negative regulator of iron deficiency
AT3G53620	PPA4	Pyrophosphatase	Regulate pyrophosphate levels
AT5G40780	LHT1	Transmembrane	High-affinity transporter for cellular amino acid uptake
AT5G03150	JKD	Zinc finger	Epidermal patterning in root meristem

Table 5 Genes with expression patterns similar to *VIN3* during the course of vernalization

Locus	Name	Protein domain	Reported function
AT5G44565	–	Transmembrane	–
AT5G55450	LTP4.4	–	Lipid transport and pathogen resistance
AT2G01150	RHA2B	Zinc finger	ABA signaling and drought response
AT1G63990	SPO11-2	DNA topoisomerase VI	Regulate meiotic recombination
AT3G27730	MER3	DEAD-like helicase	Required for meiotic crossover formation
AT4G12480	EARL11	Plant lipid transfer	Resistance to low temperature and fungal infection
AT4G21940	CPK15	Protein kinase	–
AT5G52290	SHOC1	Similar to XPF endonucleases	Required for class-I meiotic crossover formation
AT5G24860	FPF1	–	Regulate the competence to flowering
AT5G46600	–	Malate transporter	–

et al., 2009; Yun *et al.*, 2012; Xu *et al.*, 2013). *AHL* family members exist in nearly all plant species sequenced so far, ranging from moss to higher plants. In *Arabidopsis*, the *AHL* family contains 29 members with conserved AT-hook motifs known to bind to AT-rich DNA sequences (Zhao *et al.*, 2013; Zhao *et al.*, 2014). In addition to roles in the

regulation of flowering, *AHL* family members function in diverse aspects of plant growth and development including hypocotyl elongation, floral development and light responses (Lim *et al.*, 2007; Street *et al.*, 2008; Ng *et al.*, 2009; Xiao *et al.*, 2009; Yun *et al.*, 2012; Xu *et al.*, 2013).

AHL genes have evolved into two phylogenetic clades. Clade A are intron-less genes with only one AT-hook motif, whereas clade B are genes containing intron and one or two AT-hook motifs (Figure S2a) (Zhao *et al.*, 2013). Besides *AHL21* and *AHL22*, several other *AHL* family members also showed *FLC*-like transcriptional dynamics during vernalization as well as upregulated H3K27me3 marks (Figure S2b), including *AHL19*, *AHL20*, *AHL23*, *AHL24*, *AHL25*, *AHL27* and *AHL29*. Interestingly, all of the *FLC*-like *AHLs* belong to intron-less clade A, suggesting that clade A of *AHL* genes could be an ancient family involved in the cold response.

To confirm the biological function of *AHL* genes in vernalization further, we obtained the knockout and overexpression lines of *AHL22* to test its flowering phenotype with or without vernalization. The *ahl22* mutants were not significantly different from wild-type plants, probably due to the highly redundant functions of *AHL* family members. However, overexpression of *AHL22* in Col-0 delays flowering as Col-0 (*FRI*) without vernalization (Figure 6c), and the flowering was accelerated after 40 days of cold treatment (Figure 6c). Quantitative measurement indicated that the overexpression of *AHL22* resulted in elevated rosette leaves in Col-0 comparable with but less than that in *FRI*-Col-0 without vernalization (Figure 6c). Vernalization partially rescued the late-flowering phenotype in *AHL22* overexpression line but was less effective than that in *FRI*-Col-0 (Figure 6c), suggesting that *AHL22* might function in parallel to *FLC* in regulating downstream floral genes. Altogether, we propose that *AHL* family genes, particularly genes belonging to clade A, may be ancient yet novel floral regulators in the vernalization pathway, which were switched off by prolonged cold-induced H3K27me3 to assist the acceleration of flowering in *A. thaliana*.

DISCUSSION

To our knowledge, this work presents the first profile of dynamic transcriptome and epigenome changes during vernalization in *A. thaliana*. RNA-seq data were collected for samples without cold exposure, with 1-h, 1-, 10-, 20- and 40-day exposure to cold, and with a 40-day cold followed by 10 days at normal growth temperature. Analyses revealed six major clusters of differentially regulated genes. Plant hormone signaling genes were among those with altered expression immediately after exposure to cold. Throughout the exposure to cold, translation-related genes were upregulated to enable efficient protein synthesis when enzymatic activities were limited by low temperature. In addition, throughout the

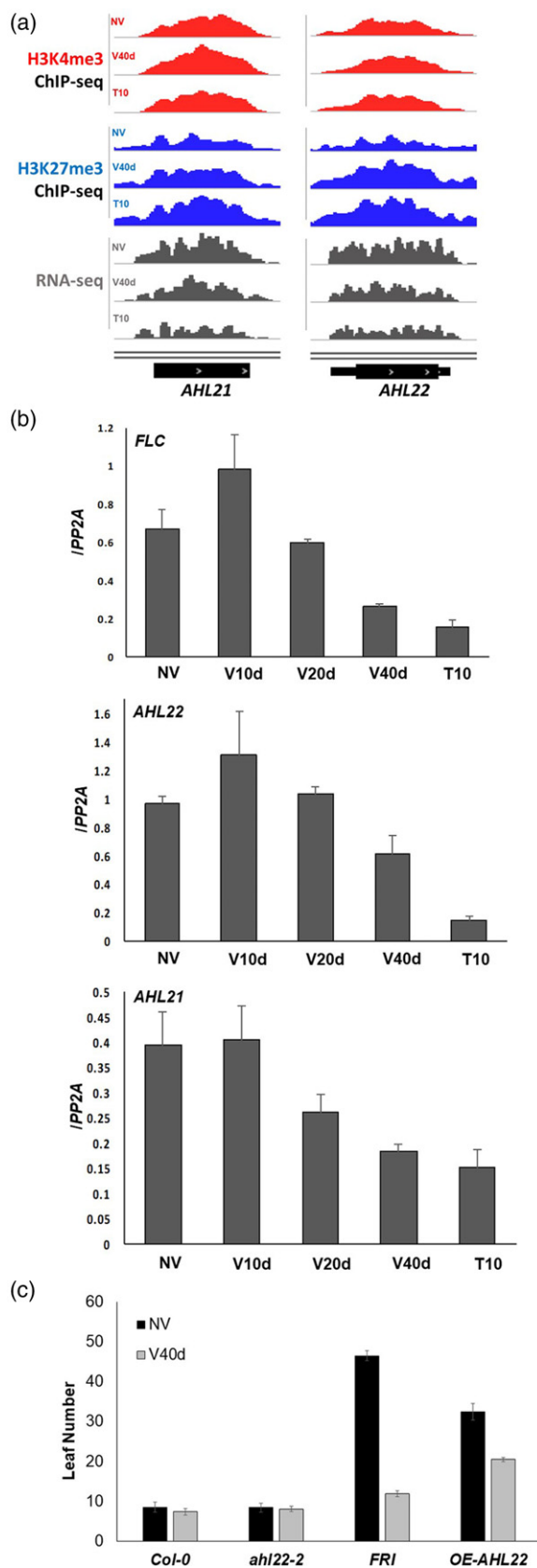


Figure 6. Phenotypes of *AHL22* knockout and overexpression strains.

(a) Genome browser tracks showing H3K4me3 (red), H3K27me3 (blue) and RNA-seq (gray) results at *AHL21* and *AHL22* loci during vernalization. NV, without cold exposure; V40d, 40-day cold; T10, 40-day cold followed by 10-day normal growth temperature.

(b) Validation of *FLC*, *AHL21* and *AHL22* expression levels using quantitative reverse transcription–polymerase chain reaction ($n = 3$).

(c) Flowering phenotypes with (V40d) or without (NV) vernalization of Col-0, *AHL22*-null mutant, *FRI*-null mutant, and *AHL22* overexpression lines based on counting rosette leaf numbers ($n = 12$).

cold exposure, photosynthesis-related genes were down-regulated to prevent photo-oxidative damage caused by excessive energy production. Potential protein-binding motifs within each cluster suggest interesting candidates for further studies.

Genome-wide profiling of histone modifications, including H3K4me3, H3K36me3 and H3K27me3, showed a temporary reduction of H3K4me3 at photosynthesis-related genes after 40 days of exposure to cold and upregulation of H3K27me3 after 40 days of cold with and without 10 days at optimal growing temperature. About one-third of the H3K27me3 peaks in all loci in the Arabidopsis genome, which are marked with H3K27me3, were vernalization regulated; most of these genes encode transcription factors and most harbor bivalent marks of both H3K4me3 and H3K27me3. In mammalian systems, bivalent histone modifications play critical roles in embryonic development and cell lineage commitment (Voigt *et al.*, 2013; Harikumar and Meshorer, 2015; Zaidi *et al.*, 2017). Little is known about the functions of bivalent marks in Arabidopsis, but our finding that thousands of genes, including a large portion of transcription factors, harbor both H3K4me3 and H3K27me3 suggest that “bivalency” may allow rapid switching of the transcription status of Arabidopsis genes critical to functions such as flowering.

The time-course patterns of transcriptome and epigenome changes allowed us to identify novel components of the vernalization pathway. A number of *FLC*- and *VIN3*-like genes were discovered through classification and pattern recognition. Among them, one *AHL* family gene was confirmed to be a repressor of flowering that was epigenetically silenced during vernalization. Additional candidates will be interesting targets for further studies.

EXPERIMENTAL PROCEDURES

Plant materials and growth conditions

The Arabidopsis Col-0 with a functional *FRI* allele was used as the wild-type strain. Standard growth conditions were 22°C with a 16-h light/8-h dark (long day) photoperiodic cycle under white fluorescent light. Seeds were surface sterilized, placed on agar medium and grown in the dark at 4°C for 3 days for stratification. For vernalization treatment, seedlings were grown for 7 days at 22°C, and then either harvested as NV or transferred to 4°C under short day (8-h light/16-h dark) for 1 h (V1h), 1 day (V1d), 10 days (V10d), 20 days

(V20d) and 40 days (V40d) of treatment. The T10 sample was kept at 4°C for 40 days followed by 10 days at 22°C before harvesting.

RNA extraction and qRT-PCR

Harvested samples were flash frozen in liquid nitrogen. Total RNA was extracted using the TRIzol/chloroform method. Extracted RNA was treated with DNase I to eliminate genomic DNA contamination. Approximately 2 µg of total RNA was used for cDNA synthesis using M-MLV reverse transcriptase (Promega, Madison, WI, USA). qRT-PCR was performed using SYBR green reaction mix (Applied Biosystems, Foster City, CA, USA) according to the manufacturer's instructions on a Vii7 Real-Time PCR system (Applied Biosystems).

Chromatin immunoprecipitation

Seedlings were crosslinked at 4°C with 1% formaldehyde solution under vacuum for 25 min. The reaction was terminated by addition of 0.125 M glycine. Crosslinked seedlings were rinsed in distilled water and then flash frozen in liquid nitrogen. ChIP was performed following the Abcam ChIP protocol (<https://www.abcam.com/protocols/chip-using-plant-samples---arabidopsis>) with minor adjustments. Aliquots of eluted DNA were used for qRT-PCR and for sequencing.

Library construction and sequencing

Ribosomal RNAs were depleted from the extracted RNA using RiboMinus Plant Kit (Thermo Fisher, Waltham, MA, USA). The polyA-enrichment procedure was omitted to capture the total RNA. Library construction was done using NEBNext Ultra Directional RNA Library Prep Kit for Illumina (NEB, Ipswich, MA, USA) following the manufacturer's instructions. Libraries were sequenced on an Illumina HiSeq2500 platform by the Genomic Sequencing and Analysis Facility at the University of Texas at Austin.

Sequence alignment and analysis

The raw reads were trimmed and quality-filtered before being aligned to the *A. thaliana* TAIR10 transcriptome by Tophat (RNA-seq) or Bowtie2 (ChIP-seq). Aligned reads were converted to digital counts using Rsubread and were analyzed using edgeR. Differentially expressed genes were identified based on $P = 0.05$ and twofold difference cut-off. Motif analysis was done by using MEME. Peaks were called by MACS2. GO analysis was done using DAVID. Clustering was done in Python using scikit-learn packages.

ACKNOWLEDGEMENTS

We wish to thank Dr Chung-Mo Park for sharing *ahl22-2* and *ahl22-OE* seeds. The authors acknowledge the Texas Advanced Computing Center (TACC; <http://www.tacc.utexas.edu>) at The University of Texas at Austin for providing High Performance Computing resources that have contributed to the research results reported within this paper. This work was supported by NIH R01GM100108 and NSF IOS 1656764 to S. S.

CONFLICT OF INTEREST

The authors declare no conflicts of interest.

AUTHOR CONTRIBUTIONS

YX, S-RP, D-HK, E-DK and SS conceived of and implemented the method, performed the experiments and data analysis. YX and SS drafted the manuscript. SS advised on

the design and implementation of the study, interpretation of results and editing the manuscript.

DATA AVAILABILITY STATEMENT

The data used in this study found at GSE 130291 (<https://www.ncbi.nlm.nih.gov/geo/query/acc.cgi?acc=GSE130291>).

SUPPORTING INFORMATION

Additional Supporting Information may be found in the online version of this article.

Figure S1. Validation of ChIP-Seq by ChIP-qPCR.

Figure S2. Characterization of *AHL* family genes.

Table S1. Summary of RNA-Seq analysis.

Table S2. Summary of ChIP-Seq analysis.

Table S3. Annotation of transcription factors with bivalent marks.

REFERENCES

- Bond, D.M., Wilson, I.W., Dennis, E.S., Pogson, B.J. and Jean Finnegan, E. (2009) VERNALIZATION INSENSITIVE 3 (VIN3) is required for the response of *Arabidopsis thaliana* seedlings exposed to low oxygen conditions. *Plant J.* **59**, 576–587.
- Chen, M. and Penfield, S. (2018) Feedback regulation of COOLAIR expression controls seed dormancy and flowering time. *Science*, **360**, 1014–1017.
- Choi, K., Kim, S., Kim, S.Y., Kim, M., Hyun, Y., Lee, H., Choe, S., Kim, S.G., Michaels, S. and Lee, I. (2005) SUPPRESSOR OF FRIGIDA3 encodes a nuclear ACTIN-RELATED PROTEIN6 required for floral repression in *Arabidopsis*. *Plant Cell*, **17**, 2647–2660.
- Coustan, V., Li, P., Strange, A., Lister, C., Song, J. and Dean, C. (2012) Quantitative modulation of polycomb silencing underlies natural variation in vernalization. *Science*, **337**, 584–587.
- Crevillen, P., Sonmez, C., Wu, Z. and Dean, C. (2013) A gene loop containing the floral repressor FLC is disrupted in the early phase of vernalization. *EMBO J.* **32**, 140–148.
- Csorba, T., Questa, J.I., Sun, Q. and Dean, C. (2014) Antisense COOLAIR mediates the coordinated switching of chromatin states at FLC during vernalization. *Proc. Natl Acad. Sci. USA*, **111**, 16160–16165.
- De Lucia, F., Crevillen, P., Jones, A.M., Greb, T. and Dean, C. (2008) A PHD-polycomb repressive complex 2 triggers the epigenetic silencing of FLC during vernalization. *Proc. Natl Acad. Sci. USA*, **105**, 16831–16836.
- Gasch, P., Fundinger, M., Muller, J.T., Lee, T., Bailey-Serres, J. and Mustrup, A. (2016) Redundant ERF-VII transcription factors bind to an evolutionarily conserved cis-motif to regulate hypoxia-responsive gene expression in *Arabidopsis*. *Plant Cell*, **28**, 160–180.
- Geraldo, N., Baurle, I., Kidou, S., Hu, X. and Dean, C. (2009) FRIGIDA delays flowering in *Arabidopsis* via a cotranscriptional mechanism involving direct interaction with the nuclear cap-binding complex. *Plant Physiol.* **150**, 1611–1618.
- Gibbs, D.J., Tedds, H.M., Labandera, A.M. et al. (2018) Oxygen-dependent proteolysis regulates the stability of angiosperm polycomb repressive complex 2 subunit VERNALIZATION 2. *Nat. Commun.* **9**, 5438.
- Gu, X., Le, C., Wang, Y., Li, Z., Jiang, D. and He, Y. (2013) *Arabidopsis* FLC clade members form flowering-repressor complexes coordinating responses to endogenous and environmental cues. *Nat. Commun.* **4**, 1947.
- Harikumar, A. and Meshorer, E. (2015) Chromatin remodeling and bivalent histone modifications in embryonic stem cells. *EMBO Rep.* **16**, 1609–1619.
- Helliwell, C.A., Wood, C.C., Robertson, M., James Peacock, W. and Dennis, E.S. (2006) The *Arabidopsis* FLC protein interacts directly in vivo with SOC1 and FT chromatin and is part of a high-molecular-weight protein complex. *Plant J.* **46**, 183–192.
- Heo, J.B. and Sung, S. (2011) Vernalization-mediated epigenetic silencing by a long intronic noncoding RNA. *Science*, **331**, 76–79.
- Hepworth, S.R., Valverde, F., Ravenscroft, D., Mouradov, A. and Coupland, G. (2002) Antagonistic regulation of flowering-time gene SOC1 by CONSTANS and FLC via separate promoter motifs. *Embo J.* **21**, 4327–4337.

- Hu, X., Kong, X., Wang, C. *et al.* (2014) Proteasome-mediated degradation of FRIGIDA modulates flowering time in Arabidopsis during vernalization. *Plant Cell*, **26**, 4763–4781.
- Jiang, D., Gu, X. and He, Y. (2009) Establishment of the winter-annual growth habit via FRIGIDA-mediated histone methylation at FLOWERING LOCUS C in Arabidopsis. *Plant Cell*, **21**, 1733–1746.
- Johanson, U., West, J., Lister, C., Michaels, S., Amasino, R. and Dean, C. (2000) Molecular analysis of FRIGIDA, a major determinant of natural variation in Arabidopsis flowering time. *Science*, **290**, 344–347.
- Kim, D.H. and Sung, S. (2017) Vernalization-triggered intragenic chromatin loop formation by long noncoding RNAs. *Dev. Cell*, **40**, 302–312.e4.
- Kim, D.H., Zografos, B.R. and Sung, S. (2010) Mechanisms underlying vernalization-mediated VIN3 induction in Arabidopsis. *Plant Signal Behav.* **5**, 1457–1459.
- Kim, S., Choi, K., Park, C., Hwang, H.J. and Lee, I. (2006) SUPPRESSOR OF FRIGIDA4, encoding a C2H2-Type zinc finger protein, represses flowering by transcriptional activation of Arabidopsis FLOWERING LOCUS C. *Plant Cell*, **18**, 2985–2998.
- Kim, S.Y., He, Y., Jacob, Y., Noh, Y.S., Michaels, S. and Amasino, R. (2005) Establishment of the vernalization-responsive, winter-annual habit in Arabidopsis requires a putative histone H3 methyl transferase. *Plant Cell*, **17**, 3301–3310.
- Lee, J. and Lee, I. (2010) Regulation and function of SOC1, a flowering pathway integrator. *J. Exp. Bot.* **61**, 2247–2254.
- Li, Z., Jiang, D. and He, Y. (2018) FRIGIDA establishes a local chromosomal environment for FLOWERING LOCUS C mRNA production. *Nat. Plants*, **4**, 836–846.
- Lim, P.O., Kim, Y., Breeze, E. *et al.* (2007) Overexpression of a chromatin architecture-controlling AT-hook protein extends leaf longevity and increases the post-harvest storage life of plants. *Plant J.* **52**, 1140–1153.
- Liu, C., Wang, C., Wang, G., Becker, C., Zaidem, M. and Weigel, D. (2016) Genome-wide analysis of chromatin packing in *Arabidopsis thaliana* at single-gene resolution. *Genome Res.* **26**, 1057–1068.
- Luo, X., Chen, T., Zeng, X., He, D. and He, Y. (2019) Feedback Regulation of FLC by FLOWERING LOCUS T (FT) and FD through a 5' FLC Promoter Region in Arabidopsis. *Mol. Plant* **12**, 285–288.
- Michaels, S.D. and Amasino, R.M. (1999) FLOWERING LOCUS C encodes a novel MADS domain protein that acts as a repressor of flowering. *Plant Cell*, **11**, 949–956.
- Michaels, S.D., Himelblau, E., Kim, S.Y., Schomburg, F.M. and Amasino, R.M. (2005) Integration of flowering signals in winter-annual Arabidopsis. *Plant Physiol.* **137**, 149–156.
- Moon, J., Suh, S.S., Lee, H., Choi, K.R., Hong, C.B., Paek, N.C., Kim, S.G. and Lee, I. (2003) The SOC1 MADS-box gene integrates vernalization and gibberellin signals for flowering in Arabidopsis. *Plant J.* **35**, 613–623.
- Myline, J.S., Barrett, L., Tessoro, F., Mesnage, S., Johnson, L., Bernatavichute, Y.V., Jacobsen, S.E., Franz, P. and Dean, C. (2006) LHP1, the Arabidopsis homologue of HETEROCHROMATIN PROTEIN1, is required for epigenetic silencing of FLC. *Proc. Natl Acad. Sci. USA*, **103**, 5012–5017.
- Ng, K.H., Yu, H. and Ito, T. (2009) AGAMOUS controls GIANT KILLER, a multifunctional chromatin modifier in reproductive organ patterning and differentiation. *PLoS Biol.* **7**, e1000251.
- Oquist, G. and Huner, N.P. (2003) Photosynthesis of overwintering evergreen plants. *Annu. Rev. Plant Biol.* **54**, 329–355.
- Questa, J.I., Song, J., Geraldo, N., An, H. and Dean, C. (2016) Arabidopsis transcriptional repressor VAL1 triggers Polycomb silencing at FLC during vernalization. *Science*, **353**, 485–488.
- Rosa, S., De Lucia, F., Myline, J.S., Zhu, D., Ohmido, N., Pendle, A., Kato, N., Shaw, P. and Dean, C. (2013) Physical clustering of FLC alleles during Polycomb-mediated epigenetic silencing in vernalization. *Genes Dev.* **27**, 1845–1850.
- Sakoe, H. and Chiba, S. (1978) Dynamic-programming algorithm optimization for spoken word recognition. *IEEE Trans. Acoust. Speech Signal Proc.* **26**, 43–49.
- Schmitz, R.J., Hong, L., Michaels, S. and Amasino, R.M. (2005) FRIGIDA-ESSENTIAL 1 interacts genetically with FRIGIDA and FRIGIDA-LIKE 1 to promote the winter-annual habit of *Arabidopsis thaliana*. *Development*, **132**, 5471–5478.
- Searle, I., He, Y., Turck, F., Vincent, C., Fornara, F., Krober, S., Amasino, R.A. and Coupland, G. (2006) The transcription factor FLC confers a flowering response to vernalization by repressing meristem competence and systemic signaling in Arabidopsis. *Genes Dev.* **20**, 898–912.
- Sheldon, C.C., Hills, M.J., Lister, C., Dean, C., Dennis, E.S. and Peacock, W.J. (2008) Resetting of FLOWERING LOCUS C expression after epigenetic repression by vernalization. *Proc. Natl Acad. Sci. USA*, **105**, 2214–2219.
- Sheldon, C.C., Rouse, D.T., Finnegan, E.J., Peacock, W.J. and Dennis, E.S. (2000) The molecular basis of vernalization: the central role of FLOWERING LOCUS C (FLC). *Proc. Natl Acad. Sci. USA*, **97**, 3753–3758.
- Shindo, C., Aranzana, M.J., Lister, C., Baxter, C., Nicholls, C., Nordborg, M. and Dean, C. (2005) Role of FRIGIDA and FLOWERING LOCUS C in determining variation in flowering time of Arabidopsis. *Plant Physiol.* **138**, 1163–1173.
- Street, I.H., Shah, P.K., Smith, A.M., Avery, N. and Neff, M.M. (2008) The AT-hook-containing proteins SOB3/AHL29 and ESC/AHL27 are negative modulators of hypocotyl growth in Arabidopsis. *Plant J.* **54**, 1–14.
- Sun, M., Qi, X., Hou, L., Xu, X., Zhu, Z. and Li, M. (2015) Gene expression analysis of Pak Choi in response to vernalization. *PLoS ONE*, **10**, e0141446.
- Sung, S. and Amasino, R.M. (2004) Vernalization in *Arabidopsis thaliana* is mediated by the PHD finger protein VIN3. *Nature*, **427**, 159–164.
- Sung, S. and Amasino, R.M. (2006) Molecular genetic studies of the memory of winter. *J. Exp. Bot.* **57**, 3369–3377.
- Sung, S., He, Y., Eshoo, T.W., Tamada, Y., Johnson, L., Nakahigashi, K., Goto, K., Jacobsen, S.E. and Amasino, R.M. (2006) Epigenetic maintenance of the vernalized state in *Arabidopsis thaliana* requires LIKE HETEROCHROMATIN PROTEIN 1. *Nat. Genet.* **38**, 706–710.
- Swiezewski, S., Liu, F., Magusin, A. and Dean, C. (2009) Cold-induced silencing by long antisense transcripts of an Arabidopsis Polycomb target. *Nature*, **462**, 799–802.
- Tamada, Y., Yun, J.Y., Woo, S.C. and Amasino, R.M. (2009) ARABIDOPSIS TRITHORAX-RELATED7 is required for methylation of lysine 4 of histone H3 and for transcriptional activation of FLOWERING LOCUS C. *Plant Cell*, **21**, 3257–3269.
- Vastenhouw, N.L. and Schier, A.F. (2012) Bivalent histone modifications in early embryogenesis. *Curr. Opin. Cell Biol.* **24**, 374–386.
- Voigt, P., Tee, W.W. and Reinberg, D. (2013) A double take on bivalent promoters. *Genes Dev.* **27**, 1318–1338.
- Wagner, E.J. and Carpenter, P.B. (2012) Understanding the language of Lys36 methylation at histone H3. *Nat. Rev. Mol. Cell Biol.* **13**, 115–126.
- Werner, J.D., Borevitz, J.O., Uhlenhaut, N.H., Ecker, J.R., Chory, J. and Weigel, D. (2005) FRIGIDA-independent variation in flowering time of natural *Arabidopsis thaliana* accessions. *Genetics*, **170**, 1197–1207.
- Whittaker, C. and Dean, C. (2017) The FLC locus: a platform for discoveries in epigenetics and adaptation. *Annu. Rev. Cell Dev. Biol.* **33**, 555–575.
- Xiao, C., Chen, F., Yu, X., Lin, C. and Fu, Y.F. (2009) Over-expression of an AT-hook gene, AHL22, delays flowering and inhibits the elongation of the hypocotyl in *Arabidopsis thaliana*. *Plant Mol. Biol.* **71**, 39–50.
- Xu, Y., Gan, E.S., He, Y. and Ito, T. (2013) Flowering and genome integrity control by a nuclear matrix protein in Arabidopsis. *Nucleus*, **4**, 274–276.
- Yang, C.Y., Hsu, F.C., Li, J.P., Wang, N.N. and Shih, M.C. (2011) The AP2/ERF transcription factor ATERF73/HRE1 modulates ethylene responses during hypoxia in Arabidopsis. *Plant Physiol.* **156**, 202–212.
- Yuan, W., Luo, X., Li, Z., Yang, W., Wang, Y., Liu, R., Du, J. and He, Y. (2016) A cis cold memory element and a trans epigenome reader mediate Polycomb silencing of FLC by vernalization in Arabidopsis. *Nat. Genet.* **48**, 1527–1534.
- Yun, J., Kim, Y.S., Jung, J.H., Seo, P.J. and Park, C.M. (2012) The AT-hook motif-containing protein AHL22 regulates flowering initiation by modifying FLOWERING LOCUS T chromatin in Arabidopsis. *J. Biol. Chem.* **287**, 15307–15316.
- Zaidi, S.K., Fritze, S.E., Gordon, J.A. *et al.* (2017) Bivalent epigenetic control of oncogene expression in cancer. *Mol. Cell Biol.* **37**, <https://doi.org/10.1128/MCB.00352-17>.
- Zhao, J., Favero, D.S., Peng, H. and Neff, M.M. (2013) *Arabidopsis thaliana* AHL family modulates hypocotyl growth redundantly by interacting with each other via the PPC/DUF296 domain. *Proc. Natl Acad. Sci. USA*, **110**, E4688–E4697.
- Zhao, J., Favero, D.S., Qiu, J., Roalson, E.H. and Neff, M.M. (2014) Insights into the evolution and diversification of the AT-hook Motif Nuclear Localized gene family in land plants. *BMC Plant Biol.* **14**, 266.